

WORKING FLUID DISTRIBUTION OF A 315 KW ORGANIC RANKINE CYCLE SYSTEM IN THE OFF-DESIGN CONDITIONS

Zhe Wu¹, Puyao Wang¹, Qingyang Han¹, Jianzhao Li^{1,*}

¹ Harbin Marine Boiler & Turbine Research Institute, Harbin 150078, China

330249263@qq.com

ABSTRACT

The research in this paper is based on a 315 kW organic Rankine cycle (ORC) system using brazed plate heat exchangers and a radial turbine. In order to study the law of distribution and change of the working fluid in the off-design conditions, this paper takes the working fluid distribution as the research target and uses the moving boundary method to establish the heat exchanger simulation model. 315 kW ORC power generation tests working with R134a were performed, and the test data is used for calculating the level of the brazed plate heat exchangers which is difficult to measure directly, and the error is within $\pm 5\%$. The working fluid distribution were obtained under different conditions of evaporator outlet superheat degree (13~21.5 °C), condenser outlet supercooling degree (4~11.5 °C) and working fluid pump flow (2~20 kg/s). Combined with the temperature distribution of the heat exchanger and the power generation of the system, the performance characteristics of the system under off-design conditions are analysed. The research results show that the change of working fluid flow rate, superheat degree and supercooling degree are all have effects on the distribution of working fluid in the system. And the influence of working fluid flow rate is the most significant. The working fluid distribution can directly reflect the working state of the heat exchanger, and the stability of the system operation. The research results provide reference for the heat exchanger design margin of the ORC power generation system, and provide guidance for the stable and safe operation of the control system.

Keywords: organic Rankine cycle; working fluid distribution; off-design condition test; moving boundary model; heat exchanger

1. INTRODUCTION

In the face of the increasing global energy costs and energy waste, effective energy conversion methods have become the focus of many researchers. The use of ORC power generation is one of the effective solutions for converting low-grade thermal energy into electrical energy. Most of the current experimental studies are based on a small ORC power generation system of several tens of kW (Galloni E et al, 2015) (Ma Z et al, 2017), however, less experimental research on high power levels, which is closer to engineering applications has been carried out. In engineering applications, stability, reliability and safety of the system are more important for power generation systems with larger power levels.

In the process of ORC power generation system test, the liquid level of the working fluid tank is an important detection index, ensuring its sufficient height can prevent the occurrence of cavitation of the working fluid pump, and the liquid level of the heat exchanger visually reflects its heat exchange capacity and effect. Since the liquid level of the plate heat exchanger is difficult to measure directly, it is often analyzed by simulation calculation. Yousefzadeh M et al. (2015) uses dynamic simulation model to analyze the distribution of system working fluid and verify it with small ORC power generation test data. Wei D et al. (2008) compared the moving boundary method with the discrete method. He believed that using the moving boundary method to model the heat exchanger is more suitable for system control.

In this paper, the experiment and theory are combined, and the ORC power generation test is carried out under different cold and heat source conditions. According to the temperature, pressure and flow measured in the test, the moving boundary method (Bonilla J et al, 2015) can be used to calculate the liquid level distribution in the heat exchanger more quickly, and the measurement results of the working

fluid tank level gauge are combined to obtain the fluid distribution of the whole working system. The feasibility of the method was verified by the test results, and the calculation error of the liquid level was within $\pm 5\%$. Finally, the factors affecting the distribution of working fluids are analyzed, and the relationship between superheat, supercooling, working fluid flow and working fluid distribution is obtained, which provides a more effective method for system control.

2. INTRODUCTION TO THE ORC TEST SYSTEM

The main equipment of the ORC power generation system tested in this study includes brazed plate heat exchanger (evaporator, preheater, condenser), centrifugal working fluid pump, working fluid tank and radial turbine. R134a is used as working fluid. The power generation is 315 kW. As Figure 1 shows, in the heating loop, water is heated by high temperature steam through a heat exchanger. The hot water is pumped into the evaporator and preheater of the ORC power generation system. In the cooling loop, the demineralized water cooled by the cooling tower exchanges heat with R134a in the condenser of the ORC power generation system.

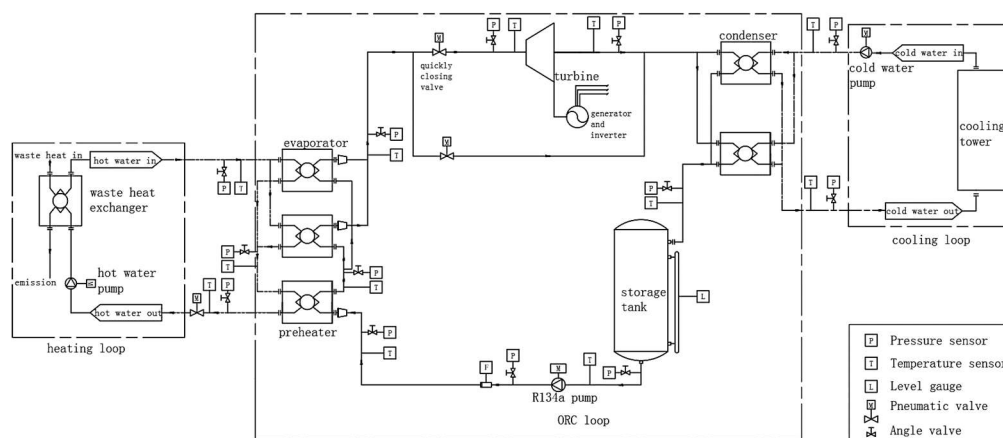


Figure 1: ORC power generation system diagram

Figure 2 is the photo of the ORC test system. In the ORC test system, the R134a working fluid is boosted into the evaporation system (evaporator and preheater) by the working fluid pump. Under the rated conditions, the vaporization process is completed in two parts. Firstly, R134a is heated to near saturation in the preheater, and then flows into the evaporator for phase change. The vaporized working fluid enters the turbine to do work, then enters the condenser to liquefy, flows into the working fluid storage tank, and finally is pumped again.

The test system is provided with temperature and pressure sensors at the inlet and outlet of each equipment, so as to monitor the working state of each equipment, and set volume flowmeter in the working fluid pump outlet, cooling water circulation pipeline and hot water circulation pipeline to measure medium flow. The measuring range and accuracy of the measuring equipment are shown in Table 1. The error bars caused by the accuracy of the sensor are shown in the figure.

Table 1: The measuring range and accuracy of the measuring equipment used in the experiment

	Pressure Sensor	Temperature Sensor	R134a flowmeter	Water flowmeter	Level gauge
Range	0-2.5 MPa	0-125 °C	0.08-1.237 m ³ /min	0-10 m ³ /min	500 mm
Accuracy	$\pm 0.25\%$	$\pm 0.25\%$	$\pm 0.963\%$	$\pm 1\%$	± 10 mm

The heat exchanger shown in Figure 3 is a vertical brazed plate heat exchanger, the water and the working medium are countercurrent heat exchange, and the evaporators and the condensers are respectively arranged in parallel, and one preheater is connected in series with the evaporators. The structural parameters of the heat exchanger are shown in Table 2 below.

The working fluid storage tank is a vertical cylinder, wherein the cross-sectional area of the liquid level change portion is 0.6 m^2 . The liquid level was measured using a magnetic flap level gauge. The working fluid pump adopts a variable frequency centrifugal pump rated at 50 Hz, and the turbine is a radial flow centering turbine.

The test system can actively control the hot water temperature, hot water flow, cooling water flow, and working fluid pump frequency, and obtain test data at different cooling water temperatures by testing in different seasons. Thus, multiple sets of test data under different design conditions are obtained.



Figure 2: Test machine photo

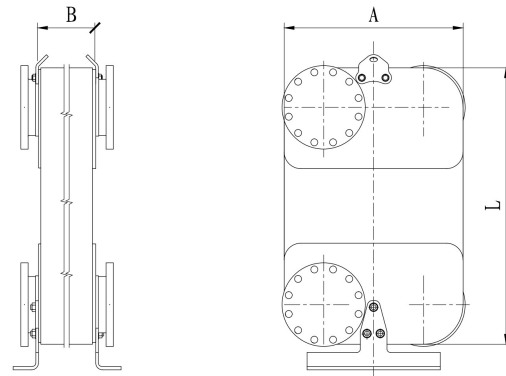


Figure 3: Plate heat exchanger

Table 2: Structural parameters of the heat exchanger

Code and meaning	Unit	Evaporator	Preheater	Condenser
L (length of the heat exchanger)	m	0.83	0.83	1.232
A (width of the heat exchanger)	m	0.537	0.537	0.537
B (thickness of the heat exchanger)	m	0.778	0.324	0.881
n (Number of plates)		300	110	400
E (equivalent plate spacing)	m	0.00219	0.00219	0.0018
F (fouling coefficient)	$\text{m}^2 \cdot ^\circ\text{C}/\text{kW}$	0.049	0.049	0.19

3. ESTABLISHMENT AND VERIFICATION OF HEAT EXCHANGER SIMULATION MODEL

3.1 Model assumptions and simplifications

In order to speed up the calculation, the model is rationally simplified based on experimental experience.

- Assume that the system is well sealed, there is no leakage and no loss of working fluid.
- The pressure drop of the plate heat exchanger is small in the test, which has little effect on the calculation of the saturation temperature point, so the model ignores the pressure drop.
- Due to the small density of the working gas, the test ignores the change of the mass distribution caused by the change of the gas density when calculating the distribution of the working fluid.
- Since the density of the working fluid changes little with temperature, the volume change caused by the change of the liquid density with temperature is ignored.

Before the test, the working fluid of the whole system is in a stable state, and the initial liquid level of each device is on the same horizontal line. For the convenience of calculation, the horizontal line is set as the initial state line. The liquid level of each equipment in the initial state is assigned, the preheater liquid level is 0.593 m, the evaporator is 0 m, the working medium tank is 0.5 m, and the condenser is 0 m. Above the initial state line, in addition to the liquid working medium in these devices, a part of the working fluid is distributed in the connecting pipe between the preheater and the evaporator and the

invalid range of the liquid level gauge in the working medium tank, and the total amount is about 0.113m³. This initial state is used to compare the liquid level distribution in the off-design conditions.

3.2 Calculation of heat transfer coefficient

For the selection of water side heat transfer coefficient, the Equation 1 is tested by a counterflow plate heat exchanger with water and refrigerant R134a on both sides. (Y-Y. Yan and T-F. Lin 1997)

$$Nu_f = 0.2121 Re_f^{0.78} Pr_f^{1/3} \left(\frac{\mu_f}{\mu_w} \right)^{0.14} \quad (1)$$

For the single-phase heat transfer coefficient of the working medium in the supercooling zone and the superheating zone, the heat exchanger correlation model modified by Dittus-Boelter is used for calculation:

$$Nu_f = 0.023 Re_f^{0.8} Pr_f^n c \quad (2)$$

When the fluid in the heat exchanger is heated, n=0.4, and when cooled, n=3.

If it is a heated gas, $c = \left(\frac{T_f}{T_w} \right)^{0.5}$.

If it is a cooled gas, $c = 1$.

If it is a heated liquid, $c = \left(\frac{\mu_f}{\mu_w} \right)^{0.11}$.

If it is a cooled liquid, $c = \left(\frac{\mu_f}{\mu_w} \right)^{0.25}$.

For the boiling heat transfer number in the evaporator, the Equation 3 obtained by Y-Y. Yan and T-F. Lin (1997) in the range of Reynolds number from 2000 to 10000 is selected:

$$Nu_f = 1.926 Pr_f^{1/3} Bo_{eq}^{0.3} Re_{eq}^{0.5} [(1-X) + X \left(\frac{\rho_f}{\rho_g} \right)^{0.5}] \quad (3)$$

In the equation:

$$G_{eq} = G [(1-X) + X \left(\frac{\rho_f}{\rho_g} \right)^{0.5}] \quad (4)$$

$$Re_{eq} = \frac{G_{eq} D_e}{\mu_f} \quad (5)$$

$$Bo_{eq} = \frac{q}{G_{eq} \gamma} \quad (6)$$

For the calculation method of condensation heat transfer coefficient in the condenser, this paper uses the calculation method proposed by Zhongzheng Wang et al. (1998)

$$Nu_f = C \left(\frac{Re_{eq}}{R} \right)^n Pr^{0.33} \left(\frac{\rho_f}{\rho_g} \right)^P \quad (7)$$

In the equation:

$$Re_{eq} = G_{eq} (1 - X_{out}) \frac{De}{\mu_f} \quad (8)$$

$$R = \frac{c_p \Delta T}{\varphi} \quad (9)$$

Combined with the above methods, Wang, L. K et al. (1999) used the test and calculation and took the mature plate heat exchanger on the market as the research object to obtain the Equation 10:

$$Nu_f = 0.0143 \left(\frac{Re_{eq}}{R} \right)^{0.864} Pr_f^{0.33} \left(\frac{\rho_f}{\rho_g} \right)^{0.055} \quad (10)$$

3.3 Solution of the heat exchange area

According to the energy conservation equation of the working side:

$$Q = m(h_{in} - h_{out}) \quad (11)$$

Energy conservation equations on the water side:

$$Q = \eta m_y C_{p_y} (T_{yout} - T_{yin}) \quad (12)$$

The energy conservation equation for heat exchange between the working fluid side and the water side:

$$S = Q \left(\frac{1}{a_{water}} + \frac{d_w}{\lambda_w} + 2F + \frac{1}{a} \right) (\Delta T_m)^{-1} \quad (13)$$

$$\Delta T_m = \frac{\Delta T_{max} - \Delta T_{min}}{\ln \frac{\Delta T_{max}}{\Delta T_{min}}} \quad (14)$$

By using the above formula for simultaneous solution, the heat exchange area of each section can be obtained, thereby obtaining the distribution of the working fluid.

3.4 Model verification

During the test, after changing the frequency of the working fluid pump, the system control variable is kept unchanged. After the working fluid flow is stabilized for a period of time, the parameter points at this time are extracted as the characteristic reference point and calculated. Using the temperature, pressure, working fluid flow rate and water flow rate of the evaporator, preheater and condenser inlet and outlet, the model can calculate the liquid level distribution of the evaporation system and the condenser during the test, such as L_{con} and L_{eva} in Figure 4.

According to the assumption that the total volume of the working medium is constant, by comparing with the liquid level of the initial heat exchanger, the liquid level distribution of the working medium tank ($L_{tank_calculation}$) can be calculated and compared with the liquid level meter measurement value ($L_{tank_measuring}$). It can be seen that during the process of frequency change of the working fluid pump, the calculated value of the liquid level of the working fluid tank is within the deviation range of $\pm 5\%$ of the measured value, which proves the accuracy and stability of the model.

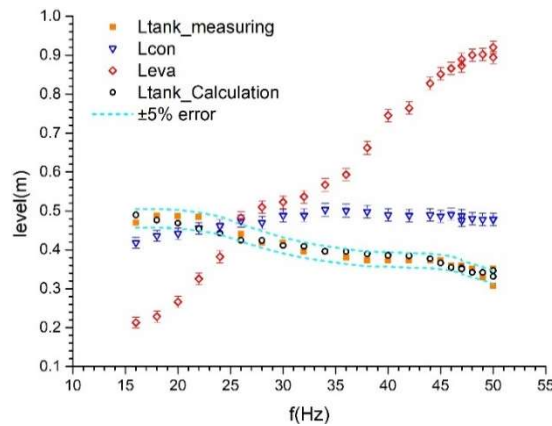


Figure 4: Comparison of calculated and measured values of system liquid level distribution

4. RESULTS AND DISCUSSIONS

The ORC power generation device was tested several times under different evaporator outlet superheat (13~21.5 °C), condenser outlet subcooling (4~11.5 °C) and working fluid pump flow rate (2~20 kg/s). Some of the data are analyzed for the distribution of working fluids.

At the beginning of the test, the gradually warming hot water enters the evaporation system. Due to the low frequency of the working fluid pump, the heat in the heating loop is relatively sufficient, and the working fluid can easily complete the phase change in the evaporation system. The evaporator has no liquid level temporarily, and the liquid level in the preheater is low too. Most of the working fluid is concentrated in the condenser and the working fluid tank. With the gradual increase of the working fluid pump frequency and the increase of the working fluid flow rate, the heat exchange area of the preheater is not enough to completely vaporize the working fluid. At about 40 Hz, the evaporator begins

to have a liquid level, the liquid level of the working fluid tank begins to decrease, and the condenser liquid level fluctuates within a small range, as shown in Figure 5 below.

As can be seen in Figure 5, under the condition that the superheat degree is about 18 °C and the degree of supercooling is about 4.5 °C, the working fluid flow rate determines the liquid level change. As the working fluid flow increases, both the evaporator and condenser levels rise. When the flow rate is increased from 9 kg/s to 18 kg/s, the evaporator liquid level is increased from 0.58 m to 0.93 m and stabilized at 0.88m. At this point, the preheater is full of working fluid, the evaporator has a liquid level of 0.05 m, and a large amount of heat exchange caused by the phase change begins to occur in the evaporator. On the other hand, the condenser has a height change of 0.06 m, and the degree of subcooling is affected by the change of the liquid level of the condenser, and there is a small range of fluctuation. This indicates that under the condition of sufficient cold source, the change of working fluid flow has little effect on the heat transfer of the condenser. In this process, the working fluid tank level drops to 0.27 m at the lowest point, a decrease of 46%. At this time, the superheat degree is 17.2 °C, the degree of subcooling is 4.6 °C, the working fluid flow rate is 16.7 kg/s, and the power generation capacity reaches 222 kW. A large amount of working fluid moves to the evaporation system, and the heat exchange area of the evaporator still has a large margin.

In another case, the test keeps the cold source condition unchanged, the subcooling degree is maintained at about 5.3 °C, the working fluid pump frequency is unchanged at 49 Hz, and the system power generation capacity reaches 315 kW. By changing the hot water temperature, the superheat of the evaporator outlet is increased from 13 °C to 21.5 °C, and the distribution of the system working fluid shown in the Figure 6 is obtained. It can be seen that the superheat is increased by 8.5 °C, so that the liquid level in the evaporation system is reduced by 0.075 m, and the phase change still occurs in the evaporator. The condenser liquid level has a small range of changes, the maximum increase of 0.028m, while the working fluid tank level increased by 0.16 m. This shows that as the degree of superheat increases, the working fluid moves toward the condenser and the working tank. Excessive superheating would waste the heat exchange area of the heat exchanger.

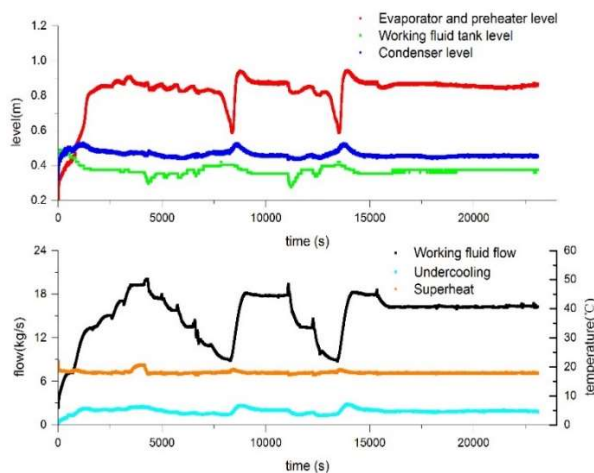


Figure 5: The change of working fluid distribution, superheat degree and supercooling degree during the change of working fluid flow

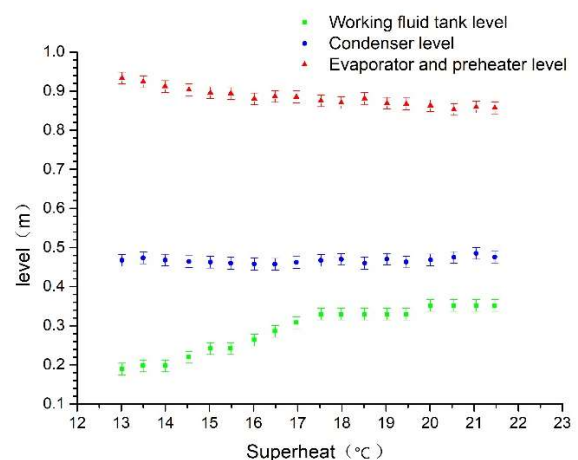


Figure 6: Effect of superheat change on working fluid distribution

On the other hand, under the condition that the working pump frequency is constant (43Hz), the distribution of the working fluid in the change of the cold source condition is analyzed by changing the cooling water flow rate (from 40kg/s to 130kg/s), as shown in Figure 7 below. As the flow rate of the cooling water increases, the outlet pressure P_{out} of the working fluid in the condenser drops significantly, which causes the pressure of the entire system to decrease. The decrease in the saturation temperature in the evaporator causes the degree of superheat ΔT_{sh} to increase and the level of the evaporation system to decrease.

The change of the condenser can be better understood by referring to Figure 8. Since the plate condenser has good heat exchange performance, the working fluid outlet temperature T_{out} (16.3 °C) is very close to the cooling water inlet temperature $T_{w,in}$ (9 °C) when the cooling water flow rate is 40 kg/s. When

the flow rate is increased to 130 kg/s, T_{out} cannot drop more (only drops 3.5°C). However, after the flow rate is increased, the pressure in the condenser is reduced by about 0.205 MPa, and the saturation temperature is reduced by 11 °C, resulting in a decrease in the degree of subcooling ΔT_{sc} from 11.5 °C to 4 °C. The heat exchange amount and the heat exchange area in the supercooled zone are reduced. The working fluid level drops. This series of changes also caused changes in turbine back pressure, which increased power generation by 66 kW and was more conducive to efficient operation of the system.

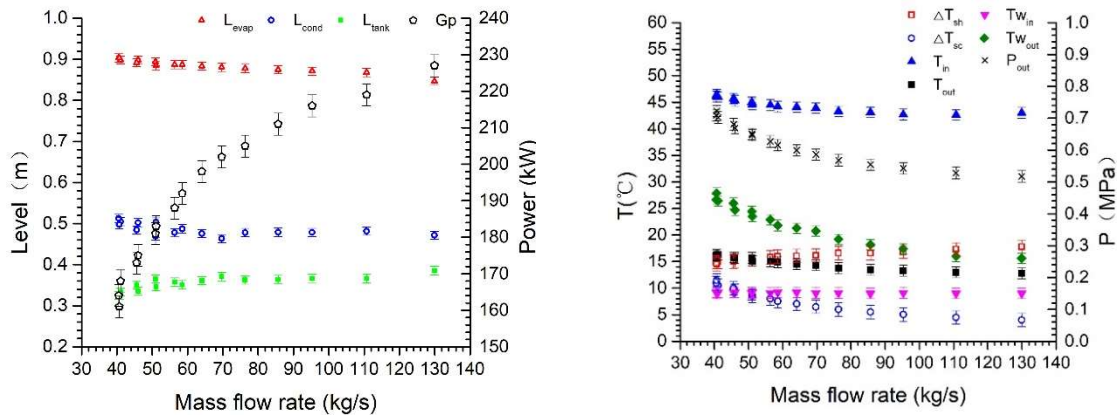


Figure 7: Operating characteristics of the condenser when the flow of cooling water changes

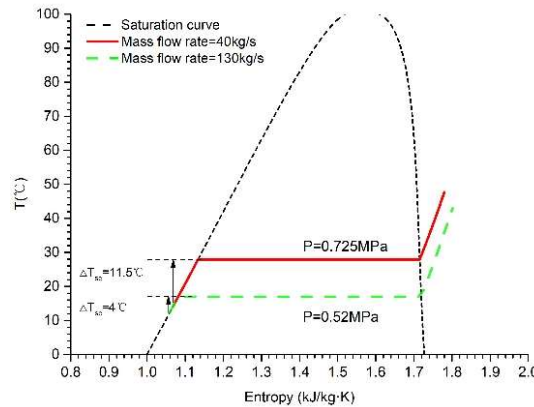


Figure 8: Temperature entropy diagram of working fluid in two states

5. CONCLUSIONS

This paper presents a new way to analyze the operating characteristics of the system in the off-design conditions. The operating characteristics of the system are analyzed by the law of liquid level change. The moving boundary method is used to calculate the heat exchange area of each phase zone of the heat exchanger, and then the liquid level distribution of the working fluid tank in the system is compared with the experimental measured value, and the error is within $\pm 5\%$. Through multiple sets of tests, the effects of working fluid flow, superheat and subcooling on the distribution of system working fluids are analyzed. The conclusions are as follows:

- The increase of the working fluid flow will significantly cause the system working fluid to move to the evaporation system side, and the sufficient evaporator design margin can ensure that the working medium is fully overheated;
- The increase of superheat degree reduces the working medium in the evaporator, and the working medium tank increases, but the influence on the condenser is relatively small, and the excessive superheat degree may cause waste of the heat exchange area of the evaporator;
- Increasing the flow rate of the cooling water causes the pressure of the condenser to drop, which causes the degree of subcooling to decrease. In this process, both the evaporator liquid level and the condenser liquid level are reduced, and the back pressure is lowered, which also greatly increases the

power generation of the system. The sufficient cooling water flow is more conducive to efficient and stable operation of the system.

- In the ORC power generation process, in order to avoid the pump cavitation caused by the emptying of the working tank, the superheat degree and the supercooling degree should be controlled within a reasonable range. The heat exchanger has enough design margin to ensure more stable and safe operation of the system when the cold and heat sources change.

NOMENCLATURE

Nu	Nusselt number	[-]	Subscript	
Re	Reynolds number	[-]	eq	Equivalent
Pr	Prandtl number	[-]	f	liquid
Bo	Boiling number	[-]	g	gas
T	Temperature	[°C]	w	water
P	Pressure	[MPa]	min	Minimum
L	Liquid level	[m]	max	maximum
Q	Heat exchange power per unit area	[W/m ²]	Con	Condenser
De	Equivalent diameter	[m]	Eva	evaporator
X	Dryness	[-]	Tank	Working fluid storage tank
c	Correction factor	[-]	sc	Subcooled
R	Dimensionless parameter	[-]	sh	Overheated
m	Mass Flow	[kg/s]		
h	Enthalpy	[J/kg]		
a	Heat transfer coefficient	[W/(m ² ·K)]		
F	Fouling coefficient	[m ² °C/kW]		
Greek symbols				
μ	Dynamic viscosity	[Pa·s]		
ρ	density	[kg/m ³]		
γ	Latent heat of vaporization	[J/kg]		
φ	Export steam dryness	[-]		
λ	Thermal Conductivity	[W/(m·K)]		
d	distance	[m]		
G	mass flux,	[kg/m ² s]		
η	energetic efficient	[-]		

ACKNOWLEDGEMENT

The authors would like to acknowledge Harbin Marine Boiler & Turbine Research Institute for the financial and technology support.

REFERENCES

- Bonilla, J., Dormido, S., & Cellier, F. E., 2015, Switching moving boundary models for two-phase flow evaporators and condensers, *Communications in Nonlinear Science & Numerical Simulation*, vol. 20, no. 3:p. 743-768.
- Galloni, E., Fontana, G., & Staccone, S., 2015, Design and experimental analysis of a mini orc (organic rankine cycle) power plant based on r245fa working fluid, *Energy*, vol. 90, :p. 768-775.
- Ma, Z. , Bao, H. , & Roskilly, A. P., 2016, Dynamic modelling and experimental validation of scroll expander for small scale power generation system, *Applied Energy*, vol. 186:p. 262-281.

- Wei, D., Lua, X., Zhen, L., & Gua, J., 2008, Dynamic modeling and simulation of an organic rankine cycle (orc) system for waste heat recovery, *Applied Thermal Engineering*, vol. 28, no. 10:p. 1216-1224.
- Yousefzadeh, M., & Uzgoren, E. , 2015, Mass-conserving dynamic organic rankine cycle model to investigate the link between mass distribution and system state, *Energy*, vol. 93, no.1:p. 1128-1139.
- Yan, Y. Y. , Lin, T. F. , & Yang, B. C. , 1997, Evaporation Heat Transfer and Pressure Drop of Refrigerant R134a in a Plate Heat Exchanger. *Asme Turbo Asia Conference. American Society of Mechanical Engineers.*
- ZHONG-ZHENGWANG, & ZHEN-NANZHAO., 1993), Analysis of performance of steam condensation heat transfer and pressure drop in plate condensers, *Heat Transfer Engineering*, vol. 14,no. 4:p. 32-41.
- Wang, L. K. , Sunden, B. , & Yang, Q. S. , 1999, Pressure drop analysis of steam condensation in a plate heat exchanger, *Heat Transfer Engineering*, vol. 20, no.1:p. 71-77.